Heliyon 10 (2024) e32690

Contents lists available at ScienceDirect

Heliyon

journal homepage: www.cell.com/heliyon

Research article

Gene expression profiling of venous malformations identifies the role of SDC1 in venous endothelial cells

Jin Li [a], Chen-Jiu Pang [b,*]

[a] Henan Provincial People's Hospital, Henan Eye Hospital, Henan Eye Institute, People's Hospital of Zhengzhou University, Zhengzhou, China
[b] Henan University People's Hospital, Zhengzhou, China

ARTICLE INFO

Keywords:
Venous malformations
Gene microarray
Syndecan-1
Differentially expressed genes
Migration
Angiogenesis

ABSTRACT

Objective: To obtain insight into the molecular process implicated in venous malformations (VMs) and identify potential targets for treatment of VMs, this study profiled the gene expression pattern in VMs, investigated alterations of syndecan-1 (SDC1) expression in VMs, and tested the hypothesis that aberrant SDC1 expression triggers abnormal angiogenesis and VM development.
Methods: Microarray analysis was performed to identify differentially expressed genes (DEGs) on a transcriptome-wide level in VMs and conjunctive normal. Gene Ontology molecular functional analysis and Kyoto Encyclopedia of Genes and Genomes pathway analysis were carried out to establish enhancement of biological signaling pathways involved in VMs. Among the DEGs, we focused on SDC1, which is involved in matrix remodeling, cell proliferation and invasion, and angiogenesis. SDC1 expression in VMs was verified by qRT-PCR, western blotting, and immunohistochemistry. Loss-of-function of SDC1 was achieved in human umbilical vein endothelial cells (HUVECs) by siRNA to investigate the roles of SDC1 in cell migration, invasion, and angiogenesis.
Results: Compared with control tissue, the transcriptome study identified 274 upregulated DEGs and 3 downregulated DEGs. The transcript and protein levels of SDC1 were significantly decreased in VMs compared with normal tissue. Inhibition of SDC1 enhanced HUVEC migration, invasion, and angiogenesis.
Conclusion: Our genome-wide microarray analysis suggests the involvement of numerous genes in VMs. Among them, SDC1 plays a substantial role in the process of angiogenesis and development of VMs. SDC1 may represent a potential target for a molecular therapy for VMs.

1. Introduction

Venous malformations (VMs) are among the most common subtypes of congenital conditions and are localized abnormalities resulting from erroneous development of the vasculature [1]. The lesions of VMs vary in type, location, and severity of the phenotype in clinical practice and contribute to swelling, pain, thrombotic complications, and morbidity. About 40 % of VMs occur in the extremities [2]. VMs are invasive, do not regress spontaneously, and tend to grow through multiple tissue levels such as skin, fat, muscle and even bone. Vascular smooth muscle cells are sparse and disordered in VMs and unable to maintain effective tension of the vascular

* Corresponding author. Henan Provincial People's Hospital, Henan Eye Hospital, Henan Eye Institute, People's Hospital of Zhengzhou University, Zhengzhou, China.
E-mail address: pangcj999@zzu.edu.cn (C.-J. Pang).

https://doi.org/10.1016/j.heliyon.2024.e32690
Received 18 May 2023; Received in revised form 29 May 2024; Accepted 6 June 2024
Available online 7 June 2024

wall. However, endothelial cells (ECs) of VMs have increased migratory and invasive abilities [3], which lead the to form tortuous venous structures that gradual expand into malformed veins. At present, treatment options include sclerotherapy, surgery, drug treatment, embolization, ablative therapies, and combination therapy, which have been unsatisfactory, especially for extensive and large VMs. Genome-level analyses in the field have been unraveling the molecular pathophysiological mechanisms and providing novel insights into new approaches and potential disease specific molecular therapies for VMs. VMs are usually sporadic and isolated, but may present with a familial pattern, which can result from inherited or somatic genetic mutations. It has been reported that the majority of isolated VMs are associated with somatic mutations of TEK, which encodes the endothelial receptor tyrosine kinase TIE2 [4]. TIE2/TEK functions via the PI3K (phosphoinositide 3-kinase)/AKT (protein kinase B)/mTOR (mammalian target of rapamycin) signaling pathway [5] and plays an important role in regulating cell proliferation, migration, and angiogenesis [6], leading to abnormal cell behavior, unbalanced quiescence, disrupted extracellular matrix (ECM) formation, decoupling of ECs and pericytes, and altered angiogenesis [6]. Most mutations detected in congenital vascular lesions play key roles in signaling pathways related to angiogenesis and vascular cell proliferation [7]. Therefore, interference with the process of angiogenesis in VMs can be a potential therapeutic option in VMs. Syndecan-1 (SDC1) is a well-studied member in the Syndecan family that is ubiquitously expressed on epithelial cells and functions in a variety of biological processes, such as cell proliferation, apoptosis, angiogenesis, tumor invasion and metastasis [8]. As a key cell surface adhesion molecule, SDC1 functions in maintaining cell morphology and interacting with the surrounding microenvironment [9]. Existing studies have shown that the SDC1 gene plays an important role in the development of organisms as well as the occurrence and progress of tumors. SDC1 is highly expressed in breast cancer, liver cancer, pancreatic cancer, gallbladder cancer, and straight colon cancer and consequently regulates the migratory ability and invasion ability of cancer cells by regulating RhoA and Rac activities [10]. SDC1 can act as a co-receptor for various heparin-binding growth factors, including basic fibroblast growth factor (bFGF/FGF2), vascular endothelial growth factor (VEGF), transforming growth factor beta (TGF-β), and platelet-derived growth factor (PDGF) [11–13] to drive growth factor signaling, and promotes tumor growth, proliferation, angiogenesis and osteolysis [14]. Angiogenesis is an essential biological process in VM progression. In view of a particular role of SDC1 in vascular cell migration, invasion, and angiogenesis, targeting SDC1 may be a potential molecular therapy for VMs. However, few studies have investigated the relationship between VMs and SDC1, and the expression of SDC1 in VMs and its role in EC migration, invasion, and angiogenesis in VMs remain unknown.

The present study aimed to profile the gene expression pattern in VMs using unbiased transcriptomic approaches, and to identify the differentially expressed genes (DEGs), functional enrichment, and related signaling pathways using in-depth bioinformatic analysis to decipher the molecular mechanisms underlying the pathogenesis of VMs. SDC1 was identified as one of the most significantly regulated genes in VMs. We hypothesized that SDC1 is involved in EC migration, invasion, and angiogenesis, and plays a key role in VMs.

Table 1
Basic information and clinical data characteristics of patients with VMs.

No	Age (years)	Gender	Location of VM	Therapy
1	17	Female	Right thigh	None
2	21	Male	Left thigh	Excision
3	11	Female	Right calf	None
4	1	Male	Right calf	None
5	28	Male	Left calf	None
6	20	Male	Right forearm	None
7	9	Male	Left thigh	None
8	5	Female	Left forearm	None
9	25	Female	Left forearm	Excision
10	22	Female	Right calf	None
11	1	Female	Right cheek	None
12	57	Male	Right cheek	None
13	4	Female	Right buttock	None
14	1	Male	Right forearm	None
15	9	Male	Left forearm	None
16	17	Female	Left forearm	None
17	1	Male	Left cheek	None
18	4	Female	Right calf	None
19	27	Female	Left thigh	Excision
20	18	Female	Right forearm	Excision
21	1	Male	Left cheek	None
22	20	Female	Left elbow	None
23	35	Female	Right buttock	Excision
24	4	Male	Right neck	None
25	4	Male	Right forearm	None
26	29	Male	Left cheek	None
27	3	Female	Left back	None
28	8	Female	Left cheek	Excision
29	21	Male	Left calf	None
30	17	Female	Left cheek	None

2. Materials and methods

2.1. Tissue sample collection

Thirty patients diagnosed with diffuse VMs who underwent surgical resection of hemangioma were recruited from the People's Hospital of Zhengzhou University from August 2019 to March 2021. During the operation, fresh VMs and normal veins located within 3 cm of the incisal margin of the lesions were collected as the experimental group and paired control group, respectively. The tissue was cut into pieces, placed in cryopreservation tubes in the operating room, and snap frozen in liquid nitrogen. Some extra VMs were retained for pathological sectioning to confirm the diagnosis. All samples were diagnosed as VMs by the Department of Pathology of the People's Hospital of Zhengzhou University. The clinicopathological features of all patients, including age, sex, region of VMs, and treatment history are presented in Table 1. This study was approved by the Ethics Committee of People's Hospital of Zhengzhou University (Ethical Approval Number: (2020) No. 119), and all samples were collected with the informed consent and written approval of the patients or their guardians.

2.2. RNA extraction

Five pairs of tissues were randomly selected from 30 pairs of tissues for microarray analysis. Total RNA was extracted from frozen tissues using the Trizol reagent (Thermo Scientific, Waltham, MA, USA). RNA was concentrated by 2-propanol and further purified using the AMBION extraction kit (Thermo Scientific). Total RNA was quantified using the NanoDrop ND-2000 (Thermo Scientific), and RNA integrity was assessed using the Agilent Bioanalyzer 2100 (Agilent Technologies Inc., Santa Clara, CA, USA).

2.2.1. Microarray experiments

The Agilent Human lncRNA Microarray 2019 (4*180 k, Design ID:086188) provided by OE Biotechnology Co. Ltd. (Shanghai, China) was used in this experiment. The sample labeling, microarray hybridization, and washing steps were performed based on the manufacturer's standard protocols. Briefly, total RNA was transcribed to double-stranded cDNA, then synthesized into cRNA and labeled with cyanine-3-CTP. The labeled cRNAs were hybridized onto the microarray. After washing, the arrays were scanned by the Agilent Scanner G2505C (Agilent Technologies Inc.).

2.3. Data analysis

Feature Extraction software (version10.7.1.1, Agilent Technologies) was used to analyze array images to obtain the raw data. GeneSpring (version 14.8, Agilent Technologies) was used to normalize the raw data and control the quality. The genes that were differentially expressed with statistical significance between VMs and adjacent normal venous tissues were identified based on criteria of an absolute fold change $\geq$2.0 and an adjusted P value $\leq$ 0.05.

2.3.1. Gene Ontology (GO) analysis and Kyoto Encyclopedia of Genes and Genomes (KEGG) pathway analysis

The molecular functional classification and related biological signaling pathways involving these DEGs were searched through GO molecular functional analysis and KEGG database signal pathway analysis.

2.3.2. SDC1 expression in human cancers in TIMER

The mRNA expression of SDC1 in different cancer types was analyzed in the Tumor IMmune Estimation Resource (TIMER) database (http://timer.cistrome.org/).

2.3.3. Cell culture and small interference RNA (siRNA) transfection

HUVECs were obtained from American Type Culture Collection (ATCC, Rockville, MD, USA) and cultured in Endothelial Cell Medium (ScienCell, San Diego, CA, USA) in an incubator containing 5 % CO_2 at 37 °C with 95 % humidity. The SDC1 siRNA sequence was designed by Hippo Biotechnology Co., Ltd. (Huzhou, Zhejiang, China). The siRNA sequence was as follows: siSDC1 sense:5′-CACCAUUCUGACUCGGUUUCUTT-3′, siSDC1 antisense:5′-AGAAACCGAGUCAGAAUGGUGTT-3'; siNC (normal control) sense: 5′-UUCUCCGAACGUGUCACGUdTdT-3′, siNC antisense: 5′-ACGUGACACGUUCGGAGAAdTdT-3'. HUVECs were inoculated on a six-well plate at a density of 1×10^5 cells/well. When cell confluency reached 80 %, HUVECs were transfected with a transfection mixture configured with 6 μl Lipo3000 and 5 μl SDC1 siRNA sequences according to the instructions for the use of Lipofectamine 3000 kits (Invitrogen, CA, USA). After culture in a 37 °C, 5 % CO_2 incubator for 6 h, the culture medium was replaced by complete medium. After 36 h, the transfection efficiency in the collected cells was detected by qRT-PCR.

2.4. Off-target effects investigation using BLAST

The Basic Local Alignment Search Tool (BLAST) was used to identify off-target matches of the SDC1 siRNA designed in the study. A BLAST search was carried out using human genomic plus transcript against the whole GeneBank database.

2.5. Quantitative reverse transcription polymerase chain reaction (qRT-PCR)

Among the screened DEGs, the SDC1 gene with a large fold change was selected, and the total RNA of tissue samples and HUVECs was extracted according to the above-mentioned method. The ReverTra Ace qPCR RT Kit (FSQ-201, Toyobo, Osaka, Japan) was used to reverse transcribe 1 μg RNA into cDNA according to the kid instructions, and qRT-PCR was carried out with SYBR Green Realtime PCR Master Mix (QPS-201, Toyobo) in a reaction volume of 20 μl. The running parameters for the StepOnePlus Real-Time PCR System were as follows: 95 °C for 60 s, 40 cycles of 95 °C for 15 s, 60 °C for 15 s, and 72 °C for 45 s. *Glyceraldehyde 3-phosphate dehydrogenase (GAPDH)* was used as an internal reference gene, and the $2^{-\Delta\Delta ct}$ method was used to calculate the relative expression levels of target genes in all samples. The mRNA primers for *GAPDH* and *SDC1* were biosynthesized by Tsingke Biotechnology Co., Ltd (Zhengzhou, China). The nucleotide sequences of the primers were as follows: SDC1-F: 5′-CCACCATGAGACCTCAACCC-3′, SDC1-R: 5′-GCCACTACAGCCGTATTCTCC-3'; GAPDH-F: 5′-GGAGTCCACTGGCGTCTTCA-3′, GAPDH-R: 5′-GTCATGAGTCCTTCCACGATACC-3'.

2.6. Western blotting

Radioimmunoprecipitation assay (RIPA) lysis buffer (Servicebio, China) containing 1 % phenylmethanesulfonyl fluoride (Servicebio) was used to extract total protein from tissue samples and HUVECs, and the BCA Protein Assay kit (Servicebio) was used to determine the protein concentration. Proteins were separated by 10 % sodium dodecyl sulfate (SDS)-polyacrylamide gel electrophoresis (PAGE) with 40 μg protein in each well. Proteins separated by electrophoretic mobility were transferred to polyvinylidene difluoride (PVDF) membranes at 300 mA for 150 min. The PVDF membranes were sealed with 5 % skim milk at room temperature for 1 h and washed the 1X Tris-buffered saline containing Tween 20 (TBST) before diluted antibody was added for overnight incubation at 4 °C. The following primary antibodies were used: anti-SDC1 (Abcam, Cambridge, UK, ab128936, 1:1000) and anti-β-actin (Wanlei, Shengyang, China, WL01372, 1:1000). On the next day, the membranes were washed with 1X TBST 3 times for 10 min each. Then, diluted fluorescent secondary antibodies were added for incubation at room temperature on a shaker for 1 h. The following secondary antibodies were used: IRDye® 800CW Goat (polyclonal) anti-rabbit IgG (LI-COR, USA, 925–32211,1:10000). The Odyssey Western Blot Detection system was used to image the blots, and ImageJ software (NIH, Bethesda, MD, USA) was used for analysis. Relative protein expression levels were analyzed using β-actin expression as an internal reference.

2.6.1. Immunohistochemistry

Sample sections were deparaffinized and rehydrated followed by antigen repair at 95 °C 1 × EDTA for 15 min. Endogenous peroxidase was blocked with 0.3 % H_2O_2-methanol for 20 min. Sections were incubated with normal serum at room temperature for 30 min and then with the primary antibody solution containing anti-human SDC1 (Abcam, Cat# ab128936) at 4 °C overnight. They were subsequently incubated with goat anti-mouse IgG secondary antibody (horseradish peroxidase [HRP] labeled] for 30 min. 3,3′-Diaminobenzidine tetrahydrochloride (DAB) was used to observe the immunostaining reaction. SDC1 expression was scored by two independent pathologists without prior knowledge of the sample information. The intensity of staining was scored as 1 (no staining), 2 (weak staining = light yellow), 3 (moderate staining = yellow brown), or 4 (strong staining = brown). The extent of staining according to the percentage of positively stained cells was scored as 1 (<25 %), 2 (25–50 %), 3 (50–75 %), or 4 (>75 %). The overall score of the staining intensity and extent of staining was defined as negative (≤2), positive (3–4), or strong positive (>4).

2.7. Scratch assay

HUVECs were added to 6-well plates at a density of 5.0×10^5/mL. Horizontal lines were drawn at the bottom of the plates at intervals of 0.5 cm, with 5 horizontal lines per well. When the cell reached 100 % confluency, the fused single layer of ECs was vertically cut with a 200-μl sterile pipette tip and gently washed with phosphate-buffered saline (PBS) three times before the addition of serum-free medium. Then, the cells were cultured at 37 °C in an incubator with 5 % CO_2 for 0, 24, or 48 h before being photographed under a microscope for comparison of migration rates. ImageJ software was used for analysis.

2.7.1. Transwell migration assay

For the Transwell migration assay, 600 μl RPMI-1640 medium containing 20 % FBS was added to the lower chambers of a 24-well plate, and then the upper Coster chambers with 8-μm pores (Corning, NY, USA) were added to avoid the formation of air bubbles between the compartment and the lower culture medium. HUVECs were re-suspended in 200 μl serum-free medium at a density of 2×10^4 cells/well and added to the upper chamber. After 36 h in culture, the liquid in the upper chamber was removed, and the nonadherent cells in the upper chamber were gently wiped off with cotton swabs. Then the cells that remained in the chamber were fixed with 4 % methanol for 20 min before staining with crystal violet for 10 min and observation under an inverted microscope. Three fields of view were randomly selected and photographed.

2.7.2. Transwell invasion assay

Matrigel (BD Biosciences, Franklin Lakes, NJ, USA) was thawed overnight in a refrigerator at 4 °C inside crushed ice. At low temperature, Matrigel was applied to the surface of the polycarbonate film in a 24-well Transwell chamber. Matrigel was prepared in a ratio of 1:8 using serum-free RPMI 1640 medium, and 600 μl of RPMI 1640 medium containing 20 % FBS was added to the lower chamber of the 24-well plate. HUVECs were re-suspended at a density of 2×10^4 cells in 200 μl serum-free medium and added to the upper chamber. After culture at 37 °C for 48 h, Matrigel and nonadherent cells in the upper chamber were wiped off, and the cells

attached to the chamber were fixed with 4 % methanol and stained with crystal violet for observation under an inverted microscope. Three fields were randomly selected and photographed.

2.7.3. Capillary tube formation assay

First, 300 μl Matrigel was added to wells of a 24-well plate and incubated at 37 °C for 1 h to allow solidification of the gel. Suspended HUVECs were then seeded in the Matrigel-coated 24-well plates at a density of 8×10^4 cells/well and incubated at 37 °C for 6 h. Then, tubule formation by HUVECs was observed and photographed under an inverted microscope. Three fields were randomly selected for statistical analysis using ImageJ software.

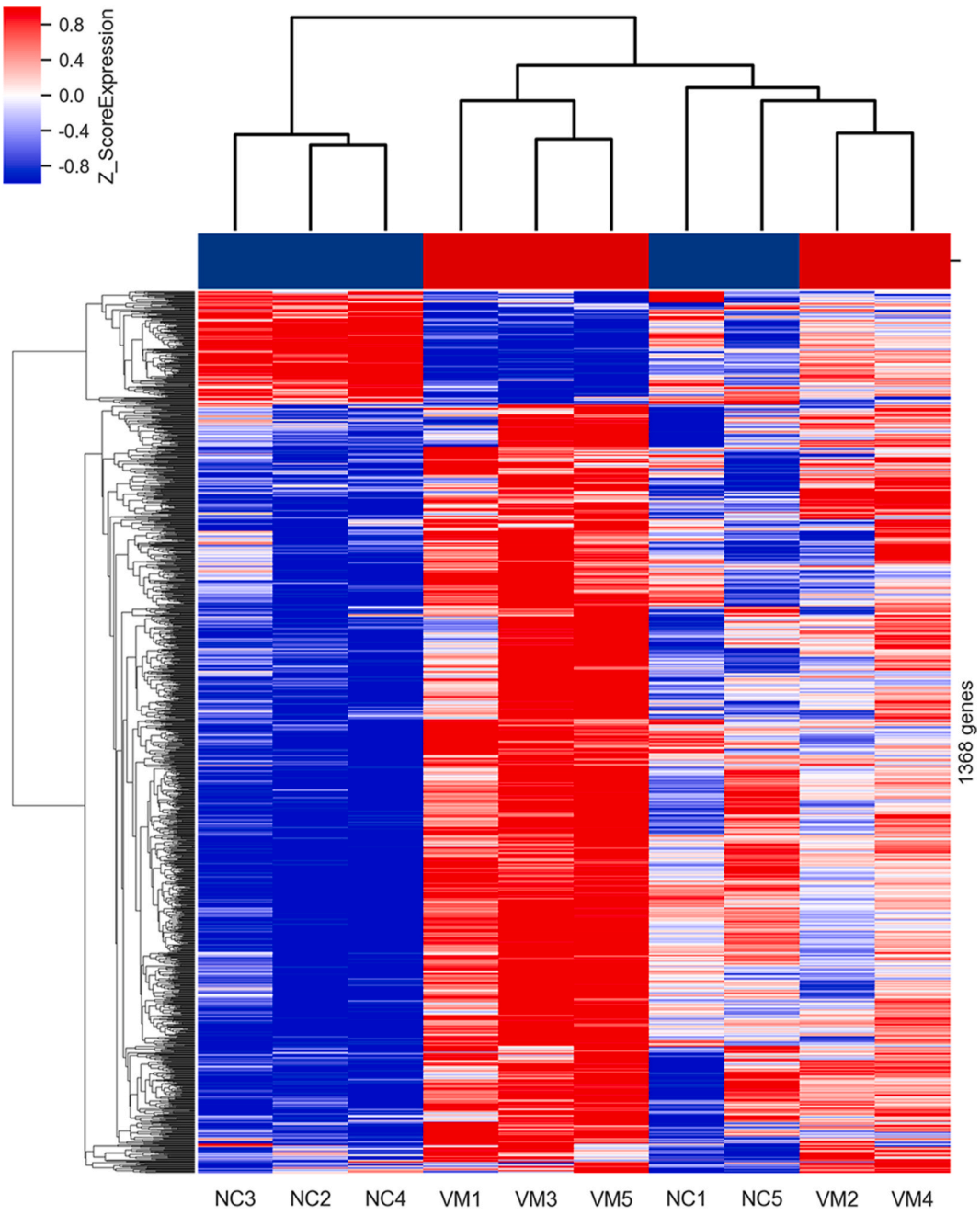

Fig. 1. Heatmap of immune-related genes that were differentially expressed between VMs and normal control tissue. Color intensity is proportional to the abundance of gene expression. Red represents upregulated genes and blue represents downregulated genes. (For interpretation of the references to color in this figure legend, the reader is referred to the Web version of this article.)

2.8. Statistical analysis

Data are expressed as the mean ± standard error of mean (SEM) from at least three independent experiments. Statistical analyses were performed using SPSS 26.0 (SPSS, Inc., Chicago, IL, USA) or Prism 8.0 (GraphPad Software, La Jolla, CA, USA). Paired *t*-test was used to compare the expression level of SDC1 in VM tissues and adjacent normal tissues. Differences between two independent groups were analyzed by independent sample *t*-test. The confidence interval was 95 %, and $P < 0.05$ was considered statistically significant.

3. Results

3.1. Differential mRNA expression profiles in VMs and normal tissues

The clinical characteristics of the enrolled VM patients are presented in Table 1. Microarray analysis was used to detect mRNA expression levels in VM tissue samples and normal control tissue samples. The screening criteria for DEGs were a false discovery rate (FDR)-adjusted $P \leq 0.05$ and fold change ≥2, and the analysis revealed 277 DEGs in the 5 pairs of tissue samples, including 274 upregulated mRNAs and 3 downregulated mRNAs (Fig. 1).

3.1.1. Functions and pathways of DEGs

The functions of DEGs were assigned to three distinct aspects of GO annotation including biological processes, cell components, and molecular functions (Fig. 2A). A total of 1282 genes were identified, among which 1055 genes were annotated by biological processes, 1108 genes were annotated by cellular component, and 1039 genes were annotated with molecular function. The most significant enrichment GO terms were 'extracellular region,' 'extracellular matrix,' and 'extracellular matrix structural constituent,' suggesting that ECM is involved in multiple cellular processes in VMs. To gain further insight into related signaling pathways, KEGG pathway analysis was performed and showed that the top three enriched pathways were complement and coagulation, protein digestion and absorption, and basal cell carcinoma (Fig. 2B). Collectively, these results suggest that various biological pathways are involved in regulating the development and progression of VMs.

3.1.2. mRNA expression level of SDC1 in pan-cancer

Microarray analysis demonstrated a significant difference in the expression of mRNA between VM tissue samples and normal control tissue samples, in which the expression of *SDC1* showed a large fold change. In view of the similarity in the biological characteristics between VMs and tumors, we further evaluated the expression of *SDC1* in pan-cancer. TIMER was used to examine the RNA sequencing data for SDC1 in TCGA. A significant increase in *SDC1* expression was found in bladder uroepithelial carcinoma, breast invasive carcinoma, cervical squamous cell carcinoma, endocervical adenocarcinoma, esophageal carcinoma, glioblastoma multiforme, head and neck squamous carcinoma-HPV positive, liver hepatocellular carcinoma, lung adenocarcinoma, lung squamous cell carcinoma, pancreatic adenocarcinoma, rectum adenocarcinoma, thyroid carcinoma, and uterine corpus endometrial carcinoma. Meanwhile, *SDC1* expression was significantly lower in renal chromophobe, renal clear cell carcinoma, renal papillary cell carcinoma, pheochromocytoma and paraganglioma, and prostate adenocarcinoma tissues than in normal tissues (Fig. 3).

3.1.3. SDC1 is downregulated in VMs

Our microarray analysis showed the abnormal expression of SDC1 in VMs. We further verified the expression of SDC1 at both the

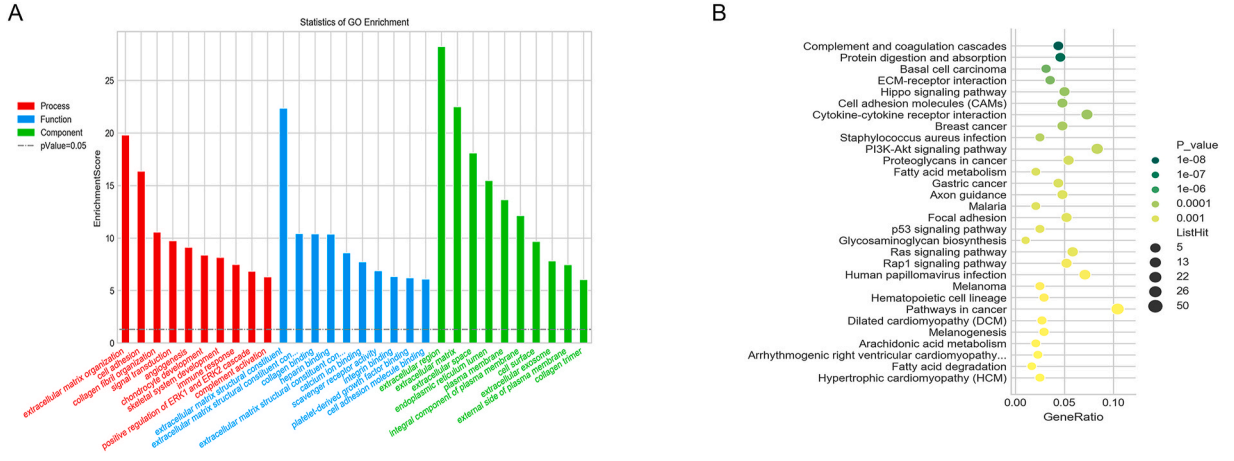

Fig. 2. GO term and KEGG pathway enrichment analyses of DEGs. A. GO annotations of DEGs were queried into 10 functional groups based on enrichment scores. B. The top 30 are presented. The enrichment factor is the ratio of the number of DEGs to the number of total genes in a particular pathway. The dot size represents the number of DEGs, while colors correspond to the range of P-values. (For interpretation of the references to color in this figure legend, the reader is referred to the Web version of this article.)

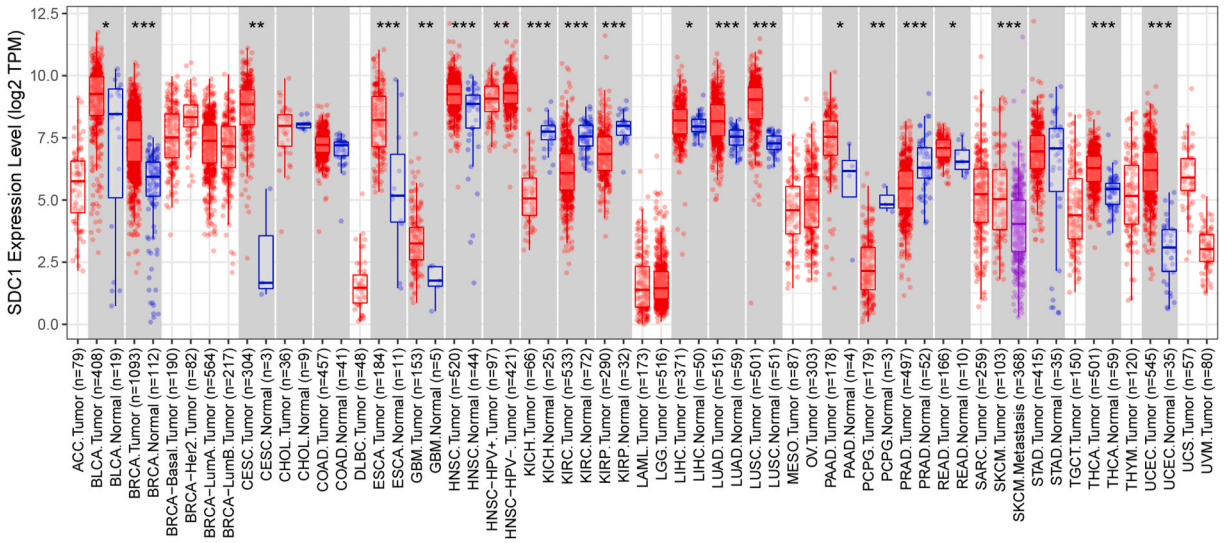

Fig. 3. SDC1 expression levels in cancers. Human SDC1 expression levels in different types of cancer from TCGA data in TIMER. *P < 0.05, **P < 0.01, ***P < 0.001.

transcript and protein levels in VMs and found that the expression levels of SDC1 mRNA and protein were significantly lower in VM tissue samples than in normal control tissue samples (Fig. 4A and B). Further immunohistochemical analysis and assessment of SDC1 expression showed SDC1 was highly expressed in the cytoplasm of ECs in normal control tissue samples, with 14 of 16 samples showing positive staining (87.50 %). Conversely, the expression of SDC1 was low or absent in VM tissue samples, with 13 of 30 samples showing positive staining (43.33 %) ($\chi^2 = 8.369$, P < 0.01) (Fig. 4C–Table 2).

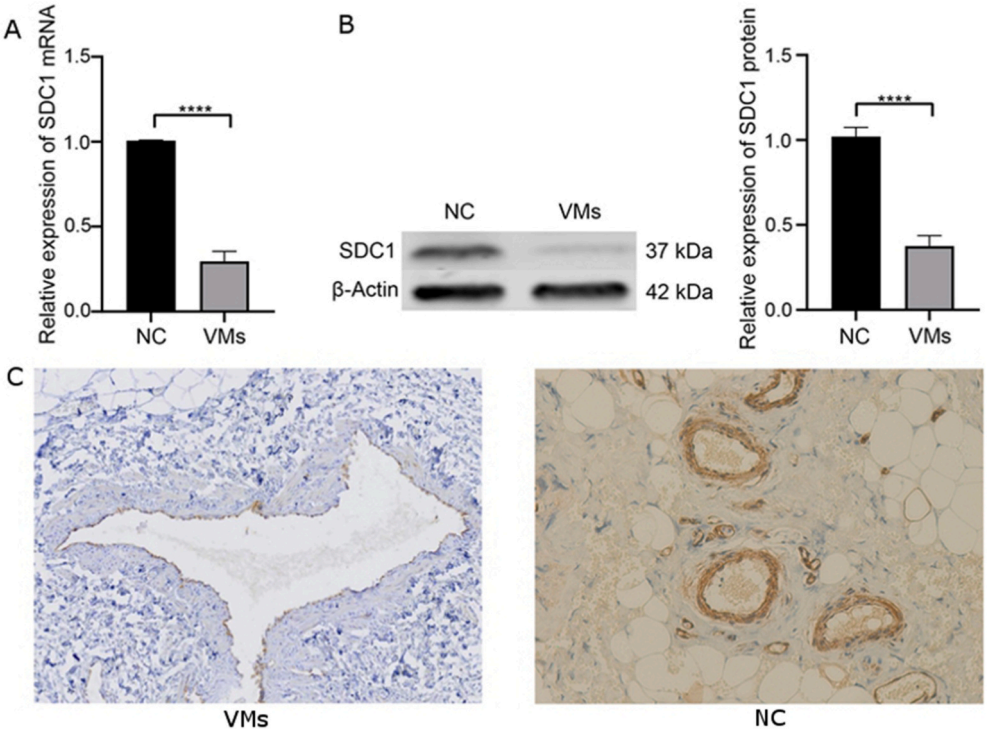

Fig. 4. mRNA and protein expression levels of SDC1 in VMs. A. Relative expression of SDC1 mRNA. B. Western blot analysis and quantification of SDC1 protein expression. ***P < 0.001. C. Immunohistochemical staining of SDC1 protein expression.

Table 2
Immunohistochemical scoring of percentage of positive SDC1 staining between VMs and NC.

Group	Cases (n)	Positive	Negative	Positive rate (%)	χ^2	P
VMs	30	13	17	43.33	8.396	<0.01
NC	16	14	2	87.50		

3.2. Loss of SDC1 function enhances the migratory and invasive abilities of HUVECs

The SDC1 siRNA sequences were subjected to BLAST analysis to search for similarity against the whole human genome, and no significant matches were found at the expect (E) threshold value of 0.005, which shows that our siRNA may not interact with any target other than SDC1. HUVECs were used to evaluate the effect of SDC1 on vascular ECs. SDC1 was silenced in HUVECs using si-SDC1, and the fluorescence expression efficiency of transfected HUVECs was very high, reaching 90 % after 36 h qRT-PCR and Western blot analyses were used to detect the gene silencing efficiency. The mRNA and protein expression levels of SDC1 in HUVECs transfected with si-SDC1 were significantly lower than those in negative control (NC) cells, indicating these cells were suitable for use in subsequent experiments (Fig. 5A and B). To investigate the effect of SDC1 on the migration of HUVECs, we performed scratch and Transwell assays to detect changes in HUVEC behaviors after SDC1 gene silencing. The results of the scratch and Transwell migration assays showed that the cells transfected with si-SDC1 healed faster than those in the normal control group, and the number of migrating cells in the si-SDC1 group was higher than that in the normal control group. The results of the Transwell invasion assay showed that the number of cells that migrated to the lower side of the Transwell chamber in the si-SDC1 group was higher than that in normal control group after 36 h in culture (Fig. 6A). These results suggest that silencing of *SDC1* improves the migratory and invasive abilities of HUVECs (Fig. 6B and C).

3.3. Loss of SDC1 function promotes angiogenesis by HUVECs

The formation of capillary-like structures by HUVECs was evaluated after silencing of *SDC1*. Total branch length, number of nodes, and number of meshes were significantly higher in the si-SDC1 group than in the negative control group, which suggests that silencing of *SDC1* enhances the ability of HUVECs to form new tube structures (Fig. 7A and B).

4. Discussion

Our study profiled genome-wide gene expression in VMs using microarray technology and found differential gene expression patterns and enrichment of signaling pathways between VMs and normal tissue. We identified for the first time *SDC1* as a novel DEG in VMs and further investigated its role in the pathogenesis of VM. Our results showed that SDC1 regulates cell migration, invasion, and angiogenesis in HUVECs. Given the lack of targeted molecular therapies for VMs, SDC1 may emerge as a promising target. Notably, our high-throughput microarray analysis established diagnostic value for DEGs and several constituents of the biological pathways involved in VMs, which has implications for patient screening, management, and ultimately clinical treatment.

More than 90 % of VMs are single-focal, and multi-focal lesions are rare [15,16]. However, in the general population, the incidence of VMs is as high as 1 % [17], and the number of patients with extensive invasive lesions is still very large. About 58 % of VMs are associated with localized intravascular coagulation (LIC) [18,19]. Prior to the discovery of the molecular mechanisms of VMs, non-surgical treatment was based primarily on management of symptoms with anticoagulant agents and pain medications to control LIC and alleviate symptoms. At present, sacrotherapy alone or combined with surgical resection is the standard treatment for VMs. Since the first somatic mutation of TEK was reported in VMs in 2009 [20], the genetic underpinnings of VMs have been gradually recognized. After identification of the PI3K/AKT/mTOR signaling pathway as an important driver within certain VMs, targeting PI3K

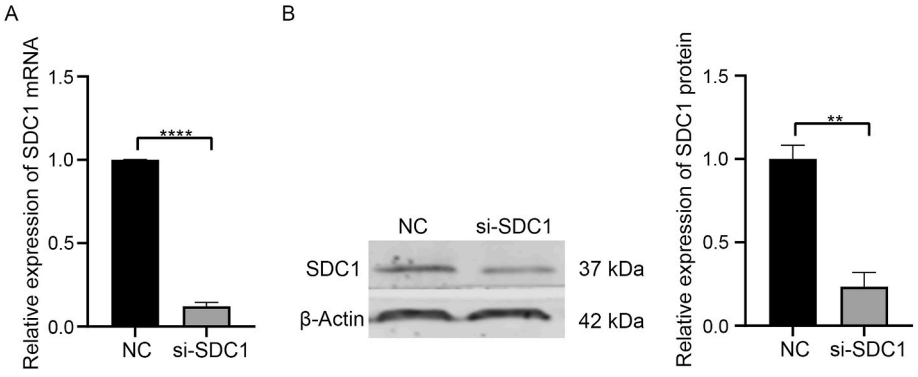

Fig. 5. Relative expression of SDC1 in HUVECs after transfection with si-SDC1. The mRNA and protein expression levels of SDC1 in HUVECs transfected with si-SDC1 were significantly lower than those in negative control cells. ***P < 0.001.

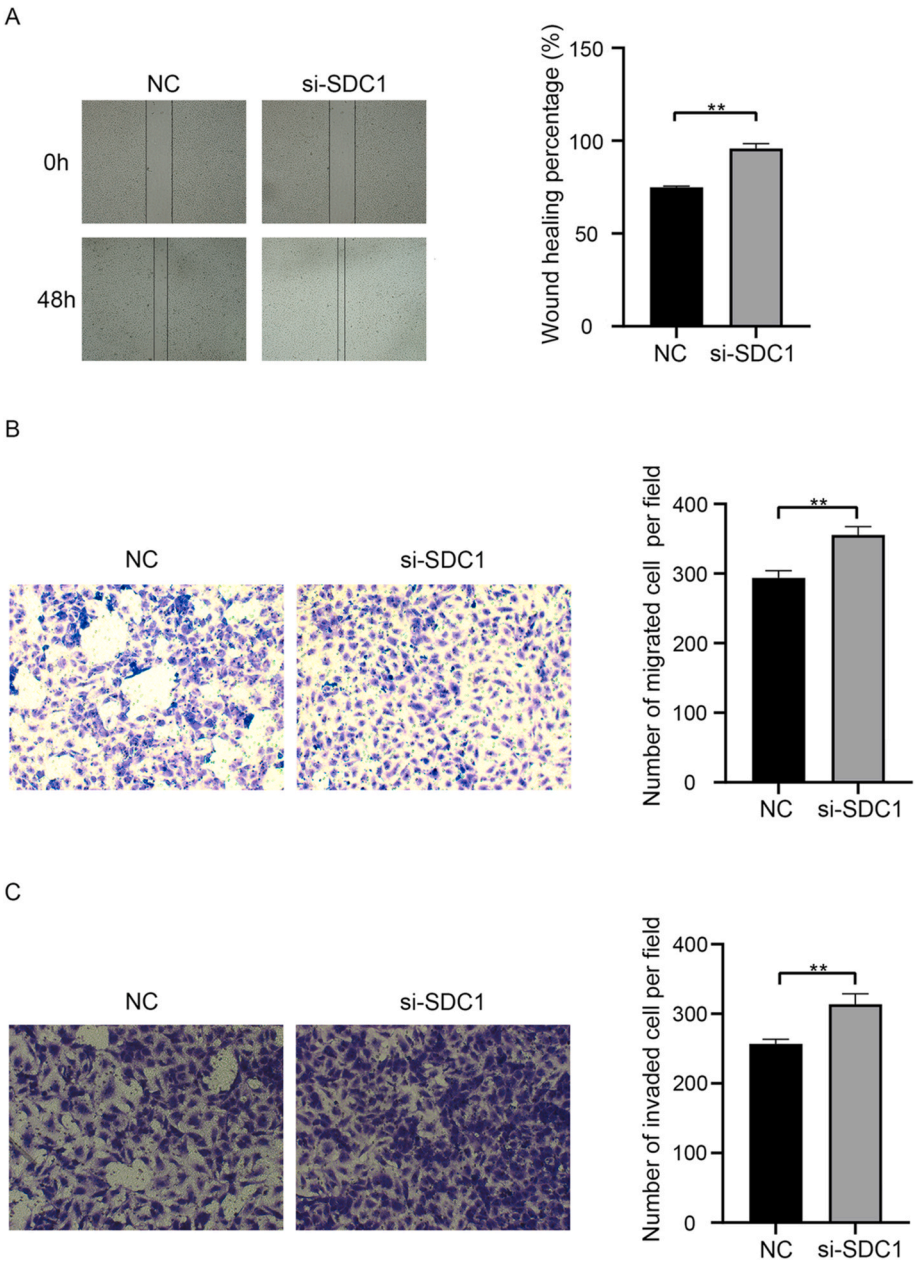

Fig. 6. Effect of SDC1 silencing on the migration and invasion of HUVECs. A. Scratch assay with HUVECs. B. Transwell migration assay with HUVECs. C. Transwell invasion assay with HUVECs. Compared with normal control (NC) group, the migration and invasion of the si-SDC1 group were increased ($\times$ 100). **P $<$ 0.01.

has become the next major therapeutic strategy for vascular anomalies (87–89). The mTOR inhibitor sirolimus became the first therapeutic target for vascular malformation and has demonstrated efficacy in reducing pain, bleeding and exudation from lesions [18, 21], the d-dimer level, and the occurrence of LIC [22], resulting in great improvement in the quality of life of patients. However, the action of sirolimus is mainly focused on preventing the development of VMs, which makes it necessary to start treatment with sirolimus as early as possible and to maintain it for life to prevent the infiltration of abnormal ECs into tissues [15,23]. Moreover, sirolimus also has safety problems such as immunosuppression, blood/bone marrow toxicity, gastrointestinal toxicity, infection, and malignancy [15, 21–23]. Therefore, future targets aimed at a different pathway need to be identified. The discoveries of new targets will likely provide more treatment strategies for patients with complex VMs.

Our microarray analysis showed differential gene expression patterns between VMs and normal control tissues. Our further functional pathway analysis revealed the enriched pathways mainly involve extracellular matrix remodeling, complement and coagulation, protein digestion and absorption, and basal cell carcinoma. Notably, we identified *SDC1* as one of the most significantly

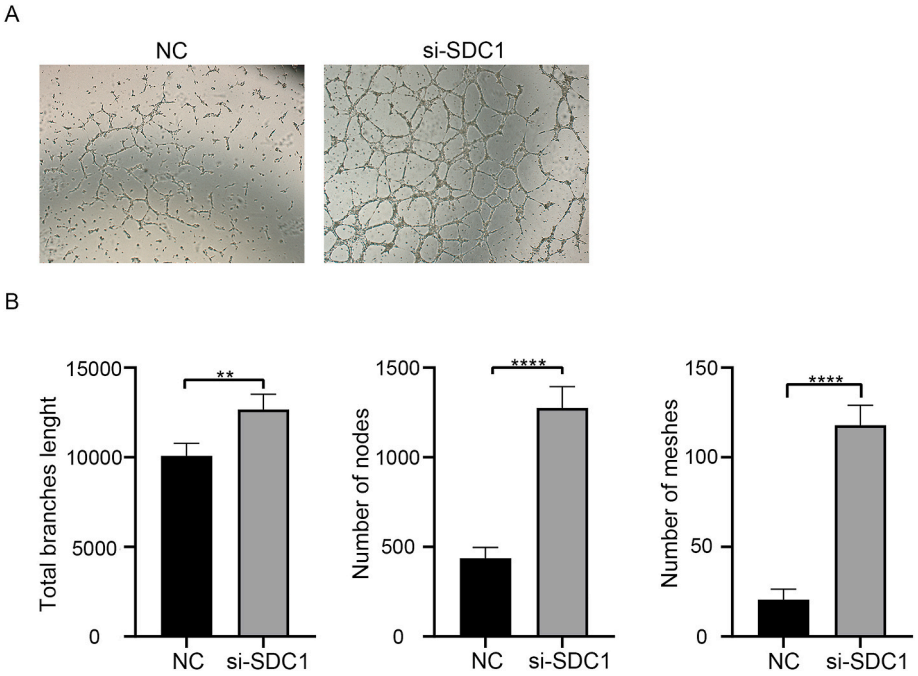

Fig. 7. Effect of SDC1 silencing on angiogenesis by HUVECs. A. Representative images of vascular networks formed by HUVECs. B. Total branch length, number of nodes, and number of meshes ($\times$ 100). **P $<$ 0.01, ***P $<$ 0.001.

dysregulated genes in VMs. The molecular function of SDC1 is highly tissue specific, which may be related to its basal level and cellular localization [23]. SDC1 regulates αVβ3 and αVβ5 integrins, which are critical in angiogenesis and tumorigenesis, and may also regulate the adhesion, diffusion, and invasion of cells expressing these integrins [24]. It has been reported that breast cancer is associated with increased SDC1 expression. In vitro breast cancer models also suggest that SDC1 is directly involved in the low diffusion and adhesion of tumor cells [25,26]. The expression of SDC1 is closely associated with the invasion and metastasis of gastric cancer [27], and the loss of epithelial SDC1 expression and decreased mesenchymal SDC1 expression in endometrial cancer patients correlate with a reduced survival rate [28]. The expression level of SDC1 in prostate cancer is negatively correlated with tumor growth [29]. Consistent with these studies, our study showed that VMs are associated with aberrant expression of SDC1, which was decreased significantly at both the transcript and protein levels in VMs compared to normal control tissue. This suggests that SDC1 may be involved in mechanisms underlying the occurrence and development of VMs.

ECs are critical in the process of venous development. Hyperactivated somatic TIE2 (encoded by TEK) and PIK3CA mutations have been identified as the primary drivers of pathological vascular growth in VMs [30]. However, the relationship between angiogenesis and SDC1 is totally unknown. Our study investigated the role of SDC1 in vascular ECs, and loss of SDC1 function in HUVECs via siRNA transfection was performed. Interestingly, we found for the first time that downregulation of SDC1 enhances the migration, invasion and angiogenesis in HUVECs, which may be associated with activation of the JAK1/STAT3 signaling pathway that was found by Fang et al. after SDC1 silencing [31]. During angiogenesis, the ECM serves essential functions in regulating EC migration, invasion, and proliferation. Our microarray analysis also showed significant enrichment of ECM in VMs. SDC1 is one of the molecules that maintain cellular spatial relationships in tissues by regulating cell–cell adhesion and cell adhesion to various ECM components. It has been shown that the invasive behavior of VMs is related to MMP-9 [3], suggesting that SDC1 may promote the invasion of VMs through MMP-9. The critical role of SDC1 in endothelial function and angiogenesis revealed by our study highlights its clinicopathological relevance in VMs. However, the novel connection between SDC1 and the related signaling pathway involved in VMs still needs to be further explored. Currently, there are several preclinical approaches targeting SDC1, such as a novel human anti-SDC1 antibody that has already shown promising results in vascular- and tumor-related disease [32–35]. Understanding the novel connection between SDC1 and the related signaling pathway involved in VMs may provide better targeted molecular therapy for patients with VMs.

5. Conclusion

Our study reveals the molecular characteristics of VMs and establishes a novel role for SDC1 in regulating angiogenesis and the development of VMs. Therefore, pharmacological targeting of SDC1 might emerge as a potential molecular therapy for VMs. However, in light of the complexity of the biological functions mediated by SDC1, the mechanism of SDC1 in regulation of vascular growth signaling pathways remains unknown and is worth exploring further in translational studies.

Data availability statement

Data will be made available on request.

Funding

This work was supported by the China Zhongguancun Precision Medicine Science and Technology Foundation ([2021]018), the Basic Science Key Project of Henan Eye Hospital (21JCZD004 and 23JCQN006), and the Medical Science and Technology Project of Henan Province (SBGJ202102052).

CRediT authorship contribution statement

Jin Li: Writing – original draft, Validation, Project administration, Funding acquisition. **Chen-Jiu Pang:** Writing – original draft, Software, Methodology.

Declaration of competing interest

The authors declare that they have no known competing financial interests or personal relationships that could have appeared to influence the work reported in this paper.

Acknowledgements

None.

List of Abbreviations

VMs	venous malformations
SDC1	syndecan-1
DEGs	differentially expressed genes
HUVECs	human umbilical vein endothelial cells
ECs	endothelial cells
PI3K	phosphoinositide 3-kinase
AKT	protein kinase B
mTOR	mammalian target of rapamycin
ECM	extracellular matrix
bFGF	basic fibroblast growth factor
VEGF	vascular endothelial growth factor
TGF-β	transforming growth factor beta
PDGF	platelet-derived growth factor
TIMER	Tumor IMmune Estimation Resource
siRNA	small interference RNA

Appendix A. Supplementary data

Supplementary data to this article can be found online at https://doi.org/10.1016/j.heliyon.2024.e32690.

References

[1] S. Behravesh, et al., Venous malformations: clinical diagnosis and treatment, Cardiovasc. Diagn. Ther. 6 (2016) 557–569.
[2] A.N. Hage, et al., Treatment of venous malformations: the data, where we are, and how it is done, Tech. Vasc. Intervent. Radiol. 21 (2018) 45–54.
[3] Y. Wang, F. Qi, J. Gu, Endothelial cell culture of intramuscular venous malformation and its invasive behavior related to matrix metalloproteinase-9, Plast. Reconstr. Surg. 123 (2009) 1419–1430.
[4] J. Soblet, et al., Blue rubber bleb nevus (brbn) syndrome is caused by somatic tek (tie2) mutations, J. Invest. Dermatol. 137 (2017) 207–216.
[5] A. Fereydooni, A. Dardik, N. Nassiri, Molecular changes associated with vascular malformations, J. Vasc. Surg. 70 (2019) 314–326.e311.
[6] M. Uebelhoer, et al., Venous malformation-causative TIE2 mutations mediate an AKT-dependent decrease in PDGFB, Hum. Mol. Genet. 22 (2013) 3438–3448.
[7] A. Queisser, L.M. Boon, M. Vikkula, Etiology and genetics of congenital vascular lesions, Otolaryngol. Clin. 51 (2018) 41–53.
[8] M. Palaiologou, I. Delladetsima, D. Tiniakos, CD138 (syndecan-1) expression in health and disease, Histol. Histopathol. 29 (2014) 177–189.
[9] M.R. Akl, et al., Molecular and clinical profiles of syndecan-1 in solid and hematological cancer for prognosis and precision medicine, Oncotarget 6 (2015) 28693–28715.
[10] T. Ishikawa, R.H. Kramer, Sdc1 negatively modulates carcinoma cell motility and invasion, Exp. Cell Res. 316 (2010) 951–965.
[11] R. Gharbaran, Insights into the molecular roles of heparan sulfate proteoglycans (HSPGs-syndecans) in autocrine and paracrine growth factor signaling in the pathogenesis of Hodgkin's lymphoma, Tumor Biol. 37 (2016) 11573–11588.

[12] M. Mochizuki, et al., Growth factors with enhanced syndecan binding generate tonic signalling and promote tissue healing, Nat. Biomed. Eng. 4 (2020) 463–475.
[13] N.F. Andersen, et al., Syndecan-1 and angiogenic cytokines in multiple myeloma: correlation with bone marrow angiogenesis and survival, Br. J. Haematol. 128 (2005) 210–217.
[14] V.C. Ramani, et al., The heparanase/syndecan-1 axis in cancer: mechanisms and therapies, FEBS J. 280 (2013) 2294–2306.
[15] E. Seront, A. Van Damme, L.M. Boon, M. Vikkula, Rapamycin and treatment of venous malformations, Curr. Opin. Hematol. 26 (2019) 185–192.
[16] J. Qiao, Y. Chen, C. Dong, J. Li, Clinical significance of galectin-3 expression in malformed hepatic venous tissue, Indian J. Med. Res. 148 (2018) 728–733.
[17] S. Eifert, J.L. Villavicencio, T.C. Kao, B.M. Taute, N.M. Rich, Prevalence of deep venous anomalies in congenital vascular malformations of venous predominance, J. Vasc. Surg. 31 (2000) 462–471.
[18] Y.Y. Han, L.M. Sun, S.M. Yuan, Localized intravascular coagulation in venous malformations: a system review, Phlebology 36 (2021) 38–42.
[19] J. Qiao, et al., Efficacy of combined topical timolol and oral propranolol for treating infantile hemangioma: a meta-analysis of randomized controlled trials, Front. Pharmacol. 11 (2020) 554847.
[20] N. Limaye, et al., Somatic mutations in angiopoietin receptor gene TEK cause solitary and multiple sporadic venous malformations, Nat. Genet. 41 (2009) 118–124.
[21] E. Boscolo, et al., Rapamycin improves TIE2-mutated venous malformation in murine model and human subjects, J. Clin. Invest. 125 (2015) 3491–3504.
[22] J.M. Mack, B. Verkamp, G.T. Richter, R. Nicholas, K. Stewart, S.E. Crary, Effect of sirolimus on coagulopathy of slow-flow vascular malformations, Pediatr. Blood Cancer 66 (2019) e27896.
[23] D.M. Adams, et al., Efficacy and safety of sirolimus in the treatment of complicated vascular anomalies, Pediatrics 137 (2016) e20153257.
[24] D.M. Beauvais, B.J. Ell, A.R. McWhorter, A.C. Rapraeger, Syndecan-1 regulates alphavbeta3 and alphavbeta5 integrin activation during angiogenesis and is blocked by synstatin, a novel peptide inhibitor, J. Exp. Med. 206 (2009) 691–705.
[25] M.E. Lendorf, T. Manon-Jensen, P. Kronqvist, H.A. Multhaupt, J.R. Couchman, Syndecan-1 and syndecan-4 are independent indicators in breast carcinoma, J. Histochem. Cytochem. 59 (2011) 615–629.
[26] D.M. Beauvais, A.C. Rapraeger, Syndecan-1-mediated cell spreading requires signaling by alphavbeta3 integrins in human breast carcinoma cells, Exp. Cell Res. 286 (2003) 219–232.
[27] Y.Q. Chu, Z.Y. Ye, H.Q. Tao, Y.Y. Wang, Z.S. Zhao, Relationship between cell adhesion molecules expression and the biological behavior of gastric carcinoma, World J. Gastroenterol. 14 (2008) 1990–1996.
[28] Kodama J. Hasengaowa, T. Kusumoto, Y. Shinyo, N. Seki, Y. Hiramatsu, Prognostic significance of syndecan-1 expression in human endometrial cancer, Ann. Oncol. 16 (2005) 1109–1115.
[29] C.E. Poblete, et al., Increased SNAIL expression and low syndecan levels are associated with high Gleason grade in prostate cancer, Int. J. Oncol. 44 (2014) 647–654.
[30] S. Schrenk, J. Goines, E. Boscolo, A patient-derived xenograft model for venous malformation, J. Vis. Exp. (2020).
[31] H. Fang, H.F. Li, M.H. He, M. Yang, J.P. Zhang, HDAC3 downregulation improves cerebral ischemic injury via regulation of the sdc1-dependent jak1/stat3 signaling pathway through mir-19a upregulation, Mol. Neurobiol. 58 (2021) 3158–3174.
[32] C. Rousseau, et al., Syndecan-1 antigen, a promising new target for triple-negative breast cancer immuno-PET and radioimmunotherapy. A preclinical study on MDA-MB-468 xenograft tumors, EJNMMI Res. 1 (2011) 20.
[33] P. Orecchia, et al., A novel human anti-syndecan-1 antibody inhibits vascular maturation and tumour growth in melanoma, Eur. J. Cancer 49 (2013) 2022–2033.
[34] H. Ikeda, et al., The monoclonal antibody nBT062 conjugated to cytotoxic Maytansinoids has selective cytotoxicity against CD138-positive multiple myeloma cells in vitro and in vivo, Clin. Cancer Res. 15 (2009) 4028–4037.
[35] N.A. Espinoza-Sánchez, M. Götte, Role of cell surface proteoglycans in cancer immunotherapy, Semin. Cancer Biol. 62 (2020) 48–67.